Applied Catalysis A: General 400 (2011) 39–47

Contents lists available at ScienceDirect

Applied Catalysis A: General

journal homepage: www.elsevier.com/locate/apcata

The influence of B-doping on the catalytic performance of Cu/HMS catalyst for the hydrogenation of dimethyloxalate

Anyuan Yin, Jingwen Qu, Xiaoyang Guo, Wei-Lin Dai*, Kangnian Fan

Department of Chemistry and Shanghai Key Laboratory of Molecular Catalysis and Innovative Materials, Fudan University, Shanghai 200433, PR China

ARTICLE INFO

Article history:
Received 21 March 2011
Accepted 8 April 2011
Available online 15 April 2011

Key words:
CuB/HMS catalysts
Hydrogenation
Dimethyl oxalate
Ethylene glycol

ABSTRACT

The influence of boron introduction on the performance of 20 wt.% Cu/HMS catalysts for the catalytic hydrogenation of dimethyloxalate was systematically investigated. It is shown that the boron loading, boron source and the preparation method all have great effect on the catalytic behaviors of the catalyst. Characterization methods including N_2-physisorption, X-ray diffraction, H_2-temperature-programmed reduction, N_2O titration, NH_3 temperature-programmed desorption, and X-ray photoelectron spectroscopy were carried out to elucidate the structure evolution of the catalyst with the introduction of boron. Experimental results showed that the B_2O_3 modified catalyst prepared via the ammonia-evaporation-induced synthesis method exhibited the highest conversion and ethylene glycol selectivity because of the higher metallic copper surface area and copper dispersion. The optimum Cu/B mole ratio, which strongly affects the surface composition of the catalyst, was found to be 2/1. 100% DMO conversion and 98% EG selectivity could be obtained over the CuB/HMS(2/1) catalyst under 2.5 h^{-1} liquid hour space velocity, which is almost four times higher than that of the one without boron introduction.

1. Introduction

The chemical selective catalytic hydrogenolysis of esters is a process of considerable significance, because it represents an approach for obtaining high valued alcohols from poorly reactive and low-cost feedstocks [1]. Among them, a basic reaction is the hydrogenation of dimethyloxalate (DMO) to ethylene glycol (EG), which is of increasing importance due to the depletion of crude oil resources [2]. Therefore, development of a highly efficient catalyst is needed to meet the increasing industrial needs for EG. Many research projects have been devoted to the hydrogenation of DMO to EG since the 1970s, among which the Cu/SiO_2 catalyst was found to afford the highest yield of EG in the hydrogenation of DMO [3] and diethyl oxalate [4], due to the weak acidic and basic properties of SiO_2. Strong acid sites would induce the intermolecular dehydration of EG, whereas strong basic sites would help to catalyze the Guerbet reaction into the formation of 1,2-butanediol [5], both of which severely deteriorate the selectivity to EG. Our early studies [6,7] showed that Cu/HMS catalyst exhibited good conversion of DMO and selectivity to EG under conditions of lower liquid hour space velocity (LHSV). From an industrial standpoint, however, excellent catalysts with highly efficient catalytic performance under much higher LHSV are highly desirable in the hydrogenation of DMO.

Boron oxide is one of the additives that are widely used to modify textural and acid–base properties of metal oxides, such as Al_2O_3 [8] and TiO_2 [9], leading to an increase in the number of acid sites together with a decrease in that of basic ones. Modifying copper species with boron introduces a very interesting change in the structural and acid–base properties of the catalyst. Wu et al. [10] found that the addition of B_2O_3 to a $Cu/ZnO/Al_2O_3$ catalyst improved the catalytic performance of the catalyst for methanol synthesis after an induction period. Li and Coville [11] used boron to improve the anti-poisoning effect of Co/TiO_2 Fischer–Tropsch catalyst. They reported that the reducibility of the catalyst by hydrogen uptake decreased with increasing boron loading because the addition of boron produced stable surface oxide sites. Moon et al. [12–14] prepared titanium–boron binary oxides by the sol–gel method. They found that Pt-loaded Ti/B photocatalyst could stoichiometrically decompose water into O_2 and H_2. Also the increasing boron content could enhance the phase transition of anatase into rutile. Therefore, it is expected that boron could not only play an electron modification effect on the catalyst, but could also stabilize the crystalline phase of the support.

Based on superior ability to intensify the electron effect, the introduction of boron materials has attracted considerable recent attention as excellent materials for the photocatalysis owing to their unique surface properties as excellent materials for the degradation of organic molecular materials [15]. To the best of our knowledge, however, the modification of boron on the Cu/SiO_2 applied in the hydrogenation of ester reaction has not yet been reported. In the present work, we investigated the development of

* Corresponding author. Tel.: +86 21 55664678, fax: +86 21 55665701.
E-mail address: wldai@fudan.edu.cn (W.-L. Dai).

0926-860X/$ – see front matter © 2011 Elsevier B.V. All rights reserved.
doi:10.1016/j.apcata.2011.04.011

a new and efficient $Cu/B_2O_3/SiO_2$ system, which exhibited significantly enhanced performance for the catalytic hydrogenation of DMO to EG.

2. Experimental

2.1. Catalyst preparation

Mesoporous siliceous HMS was prepared according to a well-established procedure delineated by Tanev et al. [16] using tetraethylorthosilicate (TEOS) as silica source and dodecylamine (DDA) as template.

Boron modified Cu/HMS catalyst was prepared by the ammonia-evaporation-induced synthetic (EVI) method described as follows: 3.80 g of $Cu(NO_3)_2{\cdot}3H_2O$ was dissolved in 100 ml of deionized water; 11 ml of 28% ammonia aqueous solution was added and stirred for 30 min. Then 4.0 g of HMS support was added to the copper ammonia complex solution and the mixture was stirred for another 2 h. The initial pH of the suspension was 11–12. Then a certain amount of B_2O_3 aqueous solution (0.05 M) was added in drops into the above solution. All the above operations were carried out at room temperature. The suspension was then pretreated at 363 K to allow for the evaporation of ammonia and to decrease the pH and consequently the deposition of copper species on silica. When the pH value of the suspension was decreased to 6–7, the evaporation process was terminated. The residue was washed with deionized water three times and ethanol once followed by drying at 393 K overnight. The catalyst precursors were calcined at 723 K for 4 h, pelletized, crushed, sieved to 40–60 meshes, and denoted as CuB/HMS(*X*/*Y*), where *X* and *Y* represent the mole ratio of Cu to B. The notation of CuB/HMS(2/1) in Table 1 means copper supported on HMS with the Cu/B mole ratio of 2/1.

For comparison, the impregnated Cu-B/HMS catalyst was synthesized via the EVI method by immersing the powder in B_2O_3 solution (0.05 M); this material was denoted as CuB/HMS(2/1)-A.

To investigate the influence of the boron source, we also synthesized Cu/HMS catalyst doped with boron, which originated from KBH_4 via the EVI method. The catalyst was denoted as CuB*/HMS(2/1), which means copper supported on HMS support with Cu/B mole ratio of 2/1. In addition, the impregnated Cu/HMS catalyst by immersing in KBH_4 aqueous solution (0.05 M) was also prepared and denoted as CuK/HMS(2/1)-I.

2.2. Catalyst characterization

Nitrogen adsorption–desorption isotherms at 77 K were measured with a Micromeritics Tristar 3000 instrument; the samples were outgassed at 423 K before each measurement. The specific surface areas were calculated following the BET method. Pore size distributions were calculated by the BJH method according to the desorption isotherm branch. The small-angle X-ray diffraction (XRD) patterns below $2\theta = 6^\circ$ were recorded on a Rigaku Multiflex instrument operated at 1.5 kW, using Cu Kα radiation (1.5406 Å) at 40 kV and 40 mA. The wide-angle XRD experiments were conducted on a Bruker D8 Advance X-ray diffractometer using nickel-filtered Cu Kα radiation with angle (2θ) range of 20–80°, a scanning speed of $2^\circ\ min^{-1}$, a voltage of 40 kV, and a current of 20 mA. The full width at half maximum (FWHM) of (1 1 1) reflection of CuO was measured for calculating crystallite sizes by using the Scherrer equation.

TPR profiles were obtained on a Tianjin XQ TP5080 autoadsorption apparatus. 50 mg of the calcinated catalyst was outgassed at 473 K under Ar flow for 2 h. After cooling to room temperature under Ar flow, the in-line gas was switched to 5% H_2/Ar, and the sample was heated to 773 K at a ramping rate of 10 K min^{-1}. The H_2 consumption was monitored by a TCD detector. The specific surface area of metallic copper was measured by the adsorption and decomposition of N_2O on the surface of metallic copper using the pulse titration method as follows: $2Cu(s) + N_2O \rightarrow N_2 + Cu_2O(s)$ at 363 K with N_2 as the carrier gas. Pure nitrogen was used to detect the consumption of N_2O [17]. The specific area of metallic copper was calculated from the total amount of N_2O consumption with 1.46×10^{19} copper atoms/m^2 [18]. X-ray photoelectron spectroscopy (XPS) spectra were recorded with a PerkinElmer PHI 5000C ESCA system equipped with a hemispherical electron energy analyzer. The Mg Kα ($h\nu$ = 1253.6 eV) anode was operated at 14 kV and 20 mA. The carbonaceous C1s line (284.6 eV) was used as the reference to calibrate the binding energies (BEs). To investigate the nature of Cu species on the surface of the reduced catalysts, we also collected XPS spectra of the samples after the hydrogenation reactions.

2.3. Catalytic reaction

The catalytic hydrogenation was performed using a fixed-bed microreactor. Typically, 2.0 g of catalyst (40–60 meshes) was loaded into a stainless steel tubular reactor with the thermocouple inserted into the catalyst bed for better control of the actual pretreatment and reaction temperature. Catalyst activation was performed at 523 K for 4 h with a ramping rate of 2 K min^{-1} under 5% H_2/Ar (v/v) flow. After cooling to the reaction temperature, 15 wt.% DMO (purity >99%) in methanol and H_2 were fed into the reactor at a H_2/DMO molar ratio of 100 and a system pressure of 2.5 MPa. The reaction temperature was first set at 473 K and the room-temperature liquid space velocity (LSV) of DMO was ranged from 0.10 to 4.30 h^{-1}. The products were condensed, and analyzed on a gas chromatograph (Finnigan Trace GC ultra) fitted with an HP-5 capillary column and a flame ionization detector (FID).

3. Results and discussion

3.1. Structural and textural properties

The BET surface area, pore volume and pore diameter of the as-prepared samples are summarized in Table 1. It is found that the BET surface areas of the catalysts range from 387 to 480 $m^2\ g^{-1}$ and the pore sizes are between 3.52 nm and 3.74 nm upon varying the Cu/B ratios. The largest BET surface area could be obtained on the one with the optimized Cu/B ratio. Compared with the catalyst prepared via EVI method, the BET surface area of the catalyst synthesized via the impregnation method is lower, which could result from the large particle size of the copper species. Different boron sources could have great effects on the textual properties of the catalysts. The BET surface area of the catalyst synthesized using KBH_4 as boron precursor decreased dramatically, especially the one prepared by the impregnation method, which could be attributed also to the larger particle size of copper species. The pore volume of the direct B_2O_3 doped catalyst is relatively larger compared with the one using KBH_4 as boron precursor, which can be explained by its textural porosity. Chemisorption of N_2O indicated that the boron modified catalysts prepared by EVI method showed much higher copper dispersion and more active copper surface area. Thus the present results are in good agreement with the dispersion trend of metallic copper as determined by XPS.

Fig. 1 shows the typical N_2 adsorption–desorption isotherm of the calcined catalysts. One can see that the mesopores characteristics of the capillary condensation are present at $P/P_0 \sim 0.35$–0.70. The shape of the hysteresis loop of the N_2 adsorption–desorption did not change a lot when changing the Cu/B ratio, which indicated that introduction of boron would not affect the pore shape

Table 1
Physicochemical properties of synthesized catalysts.

Catalyst	S_{BET}[a] ($m^2\ g^{-1}$)	$S_{Cu}^{N_2O}$ ($m^2\ g_{Cu}^{-1}$)[b]	D_{pore}[c] (nm)	V_{pore}[d] ($cm^3\ g^{-1}$)	d_{Cu}[e] (nm)
Cu/HMS	443	10.8	3.55	0.43	4.1
CuB/HMS(8/1)	431	11.5	3.74	0.47	8.3
CuB/HMS(4/1)	475	13.6	3.47	0.53	8.8
CuB/HMS(2/1)	480	16.9	3.53	0.51	9.2
CuB/HMS(1/1)	428	14.1	3.52	0.45	9.4
CuB/HMS(1/2)	387	12.3	3.75	0.42	9.4
CuB*/HMS(2/1)	405	7.2	3.81	0.43	15.8
CuB/HMS(2/1)-A	384	9.6	3.63	0.33	4.7
CuK/HMS(2/1)-I	116	2.7	4.56	0.18	33.8

[a] BET specific surface area.
[b] Cu metal surface area determined by N_2O titration method.
[c] Average pore diameter.
[d] Average pore volume.
[e] Average diameter of particle size calculated from the XRD data based on Scherrer equation.

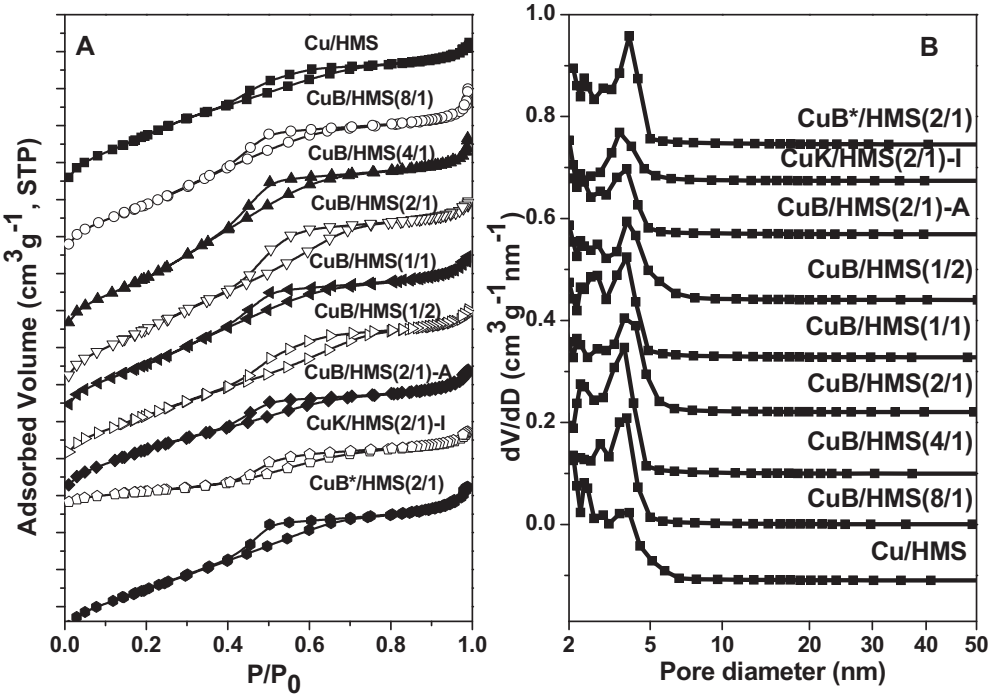

Fig. 1. N_2 sorption isotherms of the calcined catalysts (A) and BJH pore size distribution of the calcined catalysts (B).

of the support. On the other hand, the full width at half maximum of the pore size distribution decreases with increasing boron content, indicating that the pore structure became more ordered with boron introduction onto the support. In addition, a bimodal peak appeared while introducing the boron via EVI method, which might help the diffusion of the reactant molecules and the reaction heat. Other catalysts prepared by impregnation method or synthesized using KBH_4 as boron source would not generate new pores, suggesting the great influence of the preparation method and the boron sources.

To investigate the copper species of the catalysts, we collected XRD patterns of the calcined and the reduced catalysts. Fig. 2(A) shows the XRD patterns of the calcined catalysts. No obvious diffraction peaks of copper species could be observed except the sample of CuK/HMS(2/1)-I, which indicates that highly dispersed copper species could be obtained upon the EVI method and using B_2O_3 as the boron source. The peaks positioned at $2\theta = 35.5^\circ$ and 38.7° corresponded to (0 0 2) and (1 1 1) lattice planes of CuO species. The copper species segregated severely to larger particles (~24 nm) on the surface of the catalyst if the catalyst was prepared by the impregnation method using KBH_4 as the boron source. The XRD patterns of the reduced catalysts with different ratios of Cu/B are shown in Fig. 2(B). After reduction at 573 K, the peaks of copper oxides for the calcined samples disappeared, while those of metallic copper species appeared. Three main peaks positioned at $2\theta = 43.5^\circ$, 50.4° and 74.1° were corresponded to the (1 1 1), (2 0 0) and (2 2 0) lattice planes of the Cu species. The crystalline sizes of the copper species calculated based on the Scherrer equation are listed in Table 1. The particle size of Cu increased as the boron loading increased; however, the particle size did not increase further and kept constant in the range of 8.1–9.5 nm, which indicated that the boron species could stabilize the copper particle size. Fig. 2(C) shows the XRD patterns of the catalysts synthesized with different boron sources and prepared with different methods. Compared with Cu/HMS catalyst, the copper species of CuB/HMS(2/1)-A sample did not change, implying that B_2O_3 could not affect the formation and dispersion of copper species. However, the formation and dispersion of copper species could be changed during the synthesis process. After introduction of the boron species into the catalyst, the particle sizes of Cu species increased no matter what kind of boron sources (B_2O_3 or KBH_4) were used. The Cu particle sizes on the catalyst modified with B_2O_3 (9.2 nm) are smaller than

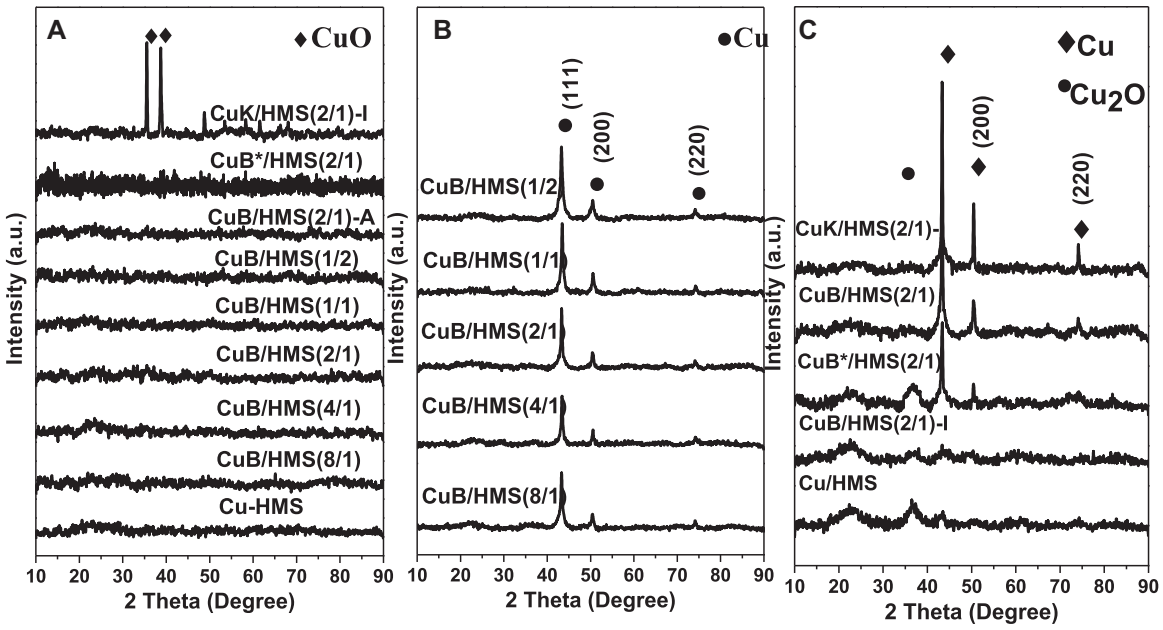

Fig. 2. XRD patterns of (A) the calcined catalysts; (B) the reduced catalysts with different mol ratios of Cu/B; (C) the reduced catalysts synthesized via different preparation methods and different boron sources.

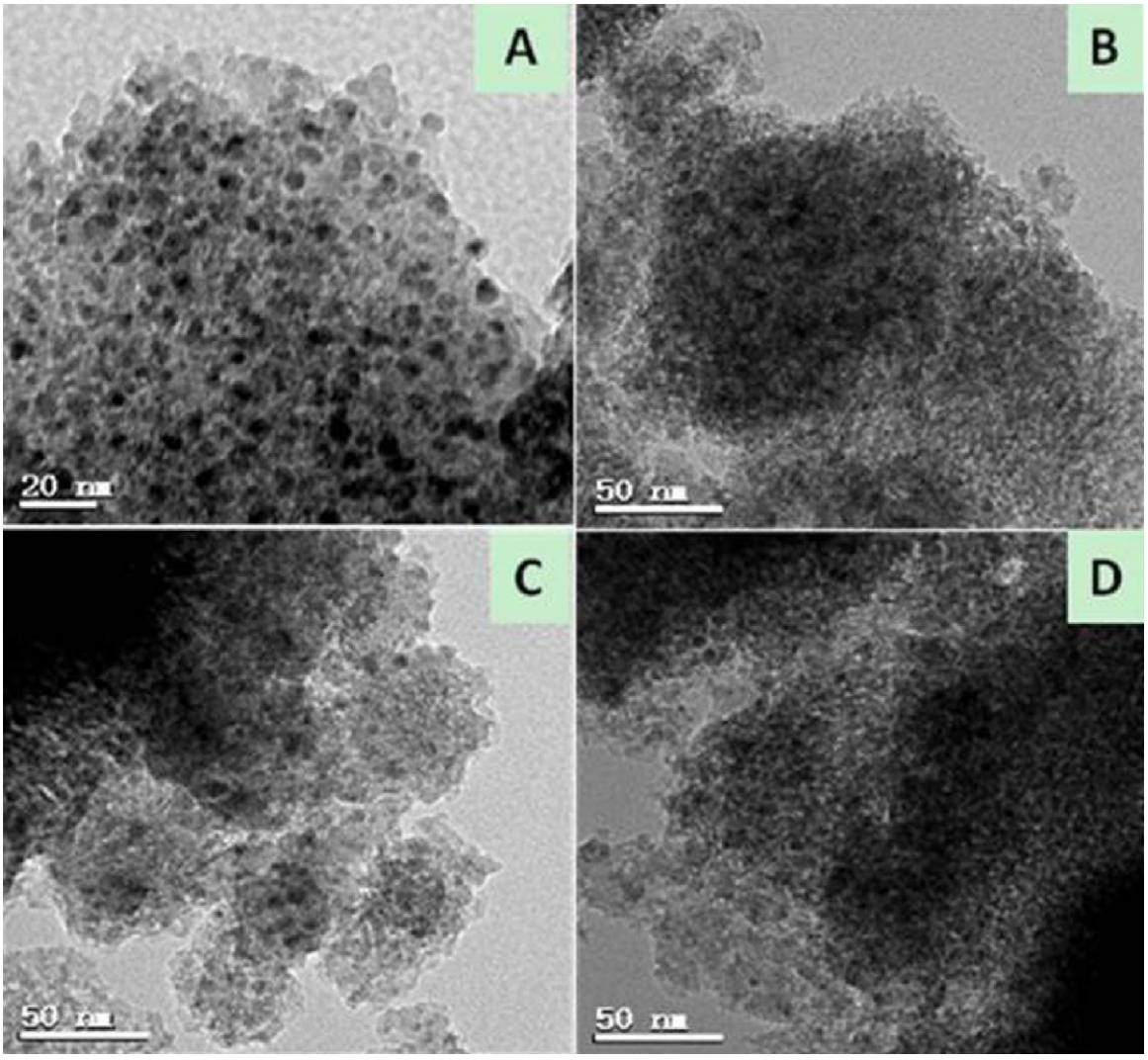

Fig. 3. TEM images of the reduced catalysts: (A) CuB/HMS(2/1), (B) CuB/HMS(2/1)-A, (C) CuB*/HMS(2/1), (D) CuK/HMS(2/1)-I.

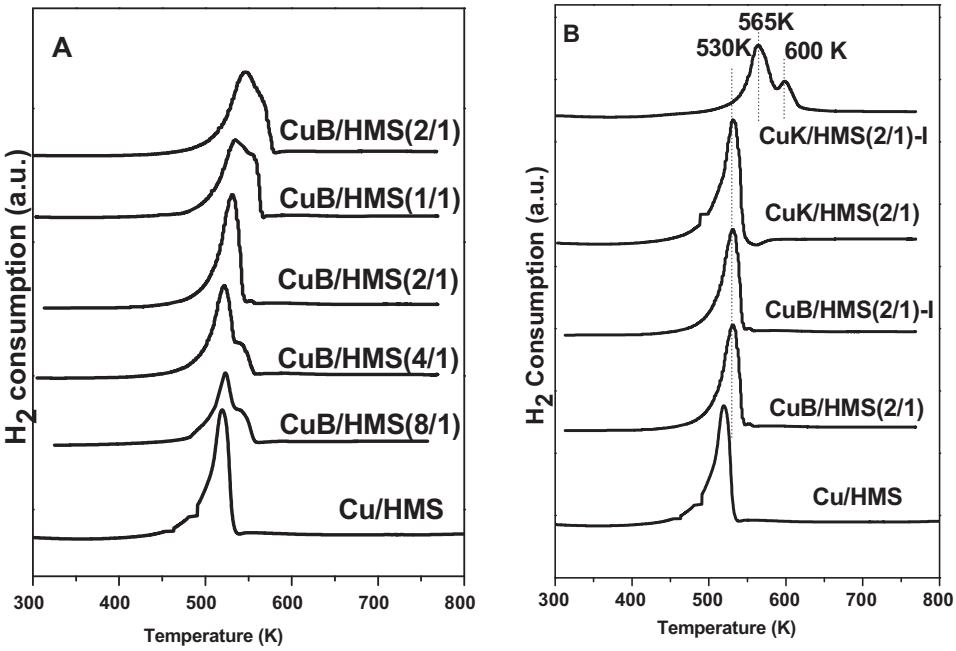

Fig. 4. TPR profiles of (A) the calcined catalysts with different ratios of Cu/B; (B) the calcined catalysts synthesized via different preparation methods and different boron sources.

those of the ones modified with KBH_4 (15.8 nm). With the same boron source, the particle size of the copper species on the catalysts prepared by EVI method is smaller than that of the one prepared by impregnated method. In addition, a diffraction peak at $2\theta = 36.8^\circ$ attributed to Cu_2O is also observed in the reduced CuB*/HMS(2/1) sample, which inferred the incomplete and inadequate reduction of Cu^{2+} species in the calcined catalysts.

Fig. 3 shows the TEM images of the four catalysts synthesized with different boron sources and prepared via different methods. One can see that, on the B_2O_3 modified sample prepared by EVI method (Fig. 3(A)), the copper particles with mostly spherical shapes were dispersed homogeneously and the average particle size is 6.4 nm. Other samples exhibited a non-homogeneous dispersion of copper species, especially for the impregnated ones. Clearly, the B_2O_3 modified catalyst could better stabilize the metal nanoparticles to limit their sizes and to promote the dispersion of copper species. In the case of the EVI derived catalyst, homogeneous $Cu(NH_3)_4(OH)_2$ species formed and were adsorbed on the surface of the support during the first step of the procedure. In the consequent dispersing and stabilizing steps, the slurry of the gel including colloidal silica together with B_2O_3 was well mixed; a highly dispersed catalyst precursor was formed. Thus by using this method one could easily obtain a catalyst precursor with small particle size and high dispersion. The TEM results were in good accordance with the observations made by XRD, TPR and XPS.

3.2. Redox behaviors

The H_2-TPR profiles of the catalysts with different Cu/B ratios and the catalysts synthesized using different boron sources and different preparation methods are illustrated in Fig. 4. The calculations of hydrogen consumption from TPR results by taking CuO as standard material showed that the practical copper content was equivalent to the theoretical value with the limits of experimental error. As can be seen, shoulders appeared in the TPR peaks of the samples with the introduction of small amounts of boron, which indicated that at least two different Cu species were present. However, along with the increase of the boron addition, the peak shoulders disappeared again. When the ratio of Cu/B is less than 2/1, peak shoulders appear again and continue to increase with the increment of the boron loading. Besides, the peak position moved positively a little on increasing the boron addition. Based on the XRD and TEM results, these two peaks could be attributed to the reduction of highly dispersed CuO with smaller and larger particle sizes respectively. Quantitatively speaking, the proportion of highly dispersed CuO with smaller particle size increased from 72% to 100%, at the same time, the proportion of CuO with larger particle size decreased from 28% to 0% with the increase of boron. The maximum proportion of highly dispersed CuO species with smaller particle size could be obtained when the ratio of Cu/B was equal to 2/1. The proper introduction amount of boron species during the synthetic procedure could affect the dispersion of the copper species as well as the interactions between copper species and silica support. Two obvious peaks appeared on the CuK/HMS-I sample, which was prepared by impregnation method using KBH_4 as boron source. The high temperature reduction peak could be attributed to the reduction of the bulk CuO, and the low temperature one could be assigned to the reduction of highly dispersed CuO species. At the same time, the peak temperature increased about 30 K compared with those of other samples, indicating that the preparation method greatly affected the dispersion of copper species. The formation of large CuO crystallites with weak or no metal-support interaction in the calcined catalyst as illustrated above is most probably due to a poor interaction between the precipitated species and the surface of the silica support. However, the copper species could disperse well upon using EVI method no matter what boron sources are used, illustrating that the EVI method played a very important role in the synthesis process.

3.3. Surface acidity

The surface acidity of the as-synthesized catalysts was measured by the NH_3-TPD method. Because of the low density and moderate strength of the active sites, the samples were flushed with nitrogen after ammonia adsorption at low temperature (393 K) before the TPD measurement. All the samples exhibited two desorption peaks, a low temperature broad peak at 373–500 K and a high one at 550–700 K, corresponding to acid sites of weak and medium

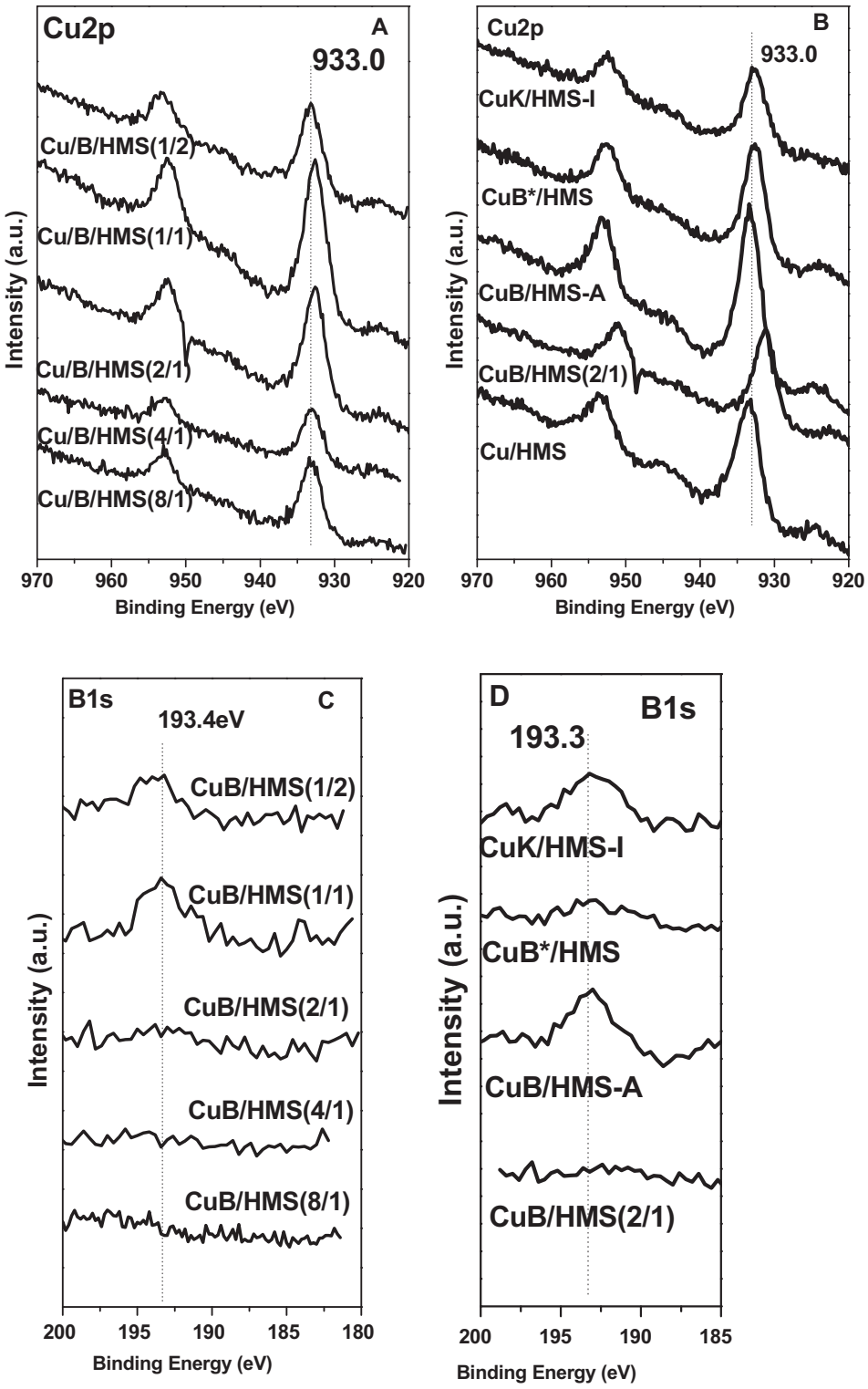

Fig. 5. Cu 2p and B1s photoelectron spectra of reduced catalysts with different mole ratios of Cu/B (A and C) and catalysts synthesized via different preparation methods and different boron sources (B and D).

strength, respectively [19]. The relative acid amounts obtained from the NH_3-TPD measurement are given in Table 2. As can be seen, the total surface acidity of the catalysts increased along with the increase of boron loading. The CuK/HMS(2/1)-I sample has the lowest amount of medium acid sites but the highest amount of weak acid sites among the catalysts, which could result from the differences of the preparation methods. Additional insight into the acid nature of the catalysts was gained from the pyridine adsorption coupled with FTIR measurements (not shown here). The results show that pyridine adsorption on the fresh catalysts was firstly carried out at room-temperature, followed by evacuation at 423 K, and gave rise to characteristic IR bands at 1542 cm^{-1}, which can be assigned to pyridine species interacting with Brønsted acid sites. No bands were observed at 1450 cm^{-1} in the spectra, indi-

Table 2
Summary of NH_3-TPD measurements.

Sample	Peak temperature (K)		NH_3-desorbed (mmol g_{cat}^{-1})		Total (mmol g_{cat}^{-1})
	α	β	α	β	
CuB/HMS(8/1)	419	608	0.03	0.02	0.05
CuB/HMS(4/1)	422	611	0.08	0.06	0.14
CuB/HMS(2/1)	438	615	0.11	0.12	0.23
CuB/HMS(1/1)	442	616	0.13	0.12	0.25
CuB/HMS(1/2)	451	614	0.18	0.18	0.36
CuB/HMS(2/1)-A	400	612	0.16	0.11	0.27
CuB*/HMS(2/1)	366	621	0.22	0.18	0.40
CuK/HMS(2/1)-I	363	638	0.24	0.03	0.27

cating that the material in the present work has no Lewis acid sites.

3.4. Chemical state and surface composition

The Cu 2p and B1s X-ray photoelectron spectra of the reduced catalysts under 5% H_2/Ar atmosphere at 573 K are presented in Fig. 5. As compared to the calcined samples, the Cu 2p3/2 BE of the reduced catalysts shifted to ca. 933.0 eV, and the 2p to 3d satellite disappeared due to the reduction of Cu^{2+}. After a careful analysis of the Cu 2p XP spectra (Fig. 5(A)), a shift to lower BE values could be detected, from 933.0 eV to 932.7 eV as the boron content in the catalysts increased. Compared with the Cu/HMS catalyst (Fig. 5(B)), introduction of boron induced the BE decrease of Cu 2p3/2, especially for the CuB/HMS(2/1) catalyst, which indicated that the boron source and the preparation method had great influence on the surface electron state of the copper species.

As can be seen from Fig. 5(C), the BE value of the B1s lies in the range of 192–194 eV, which indicated that the chemical state of boron was +3. A slight chemical shift could be observed upon varying ratios of Cu/B, the boron source and the preparation method, the differences pointing out the electron interactions between the reduced copper species and the boron species. In addition, it is worth noting that the K species only existed in the catalyst prepared by the impregnation method; no K species could be detected on other kinds of catalysts, based on the XPS survey results.

Additional insight into the relationship between the boron loading and the surface elemental ratios of Cu and B relative to Si were estimated from intensity ratios normalized by an atomic sensitivity factor. Also the ratios of B to Cu were found and were presented in Fig. 6. It can be seen that the Cu/Si ratios are lower than the bulk ones, indicating the depletion in the Cu concentration on the particle surface. The B/Cu ratios are also lower than the theoretical ones, suggesting that a certain amount of boron also came into the bulk. B/Cu ratio and B/Si ratio increased with the increase of the boron loading. The Cu/Si ratio exhibited a volcano-shaped curve as the increase of the boron loading, and the maximum Cu/Si ratio could be obtained when the ratio of Cu/B reached 2/1.

3.5. Catalytic performance

3.5.1. Effects of different mole ratios of Cu/B

DMO hydrogenation reactions were carried out to study the catalytic properties of the catalysts with different Cu/B mole ratios, and their conversion and selectivity as a function of LHSV are shown in Fig. 7(A and B). Also, to make it clear, the catalytic performance as the function of catalyst composition is given in Fig. 8. Because of a much higher dispersion of copper species, B_2O_3 modified Cu/HMS catalysts presented a much higher conversion in DMO hydrogenation. Even at higher LHSV (3.2 h^{-1}), the catalysts still showed a high conversion (100%) for the hydrogenation of DMO, suggesting that the introduction of B_2O_3 into the catalyst made the catalyst expose many more active sites or that a synergetic effect could be occurring

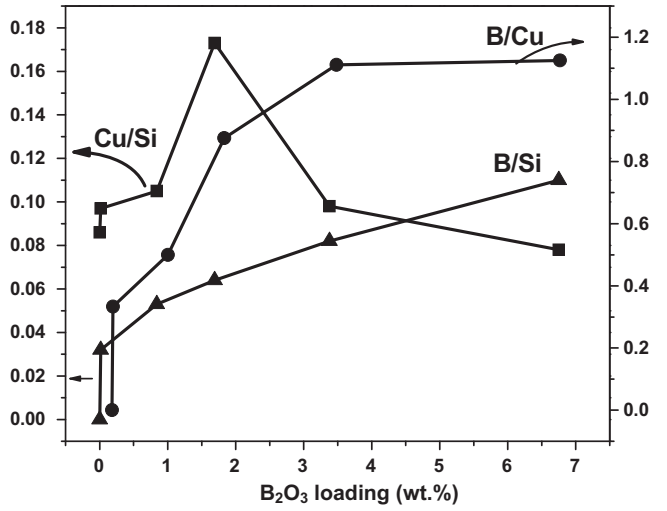

Fig. 6. Surface composition of the reduced catalysts calculated based on XPS results.

between the copper species and the boron species. Along with the increase of the boron loading, the conversion of DMO increased; the highest value could be obtained over the catalyst with Cu/B ratio of 2/1. On further increasing of the boron loading, the DMO conversion decreased, which may be due to the much higher amount of B_2O_3 on the surface that covered some active copper sites. Besides, the modification of catalyst with a proper amount of B_2O_3 species would stabilize the size of copper particles, which is the reason why the catalytic performance of all the catalysts with different ratios of Cu/B under lower LHSV condition would exhibit almost the same catalytic behavior. These results clearly show the high efficiency of the B_2O_3 modified catalyst in the hydrogenation of DMO.

The selectivity of EG could also be improved by the introduction of B_2O_3, and the EG selectivity increased along with the increase of the boron loading. The highest selectivity could be obtained over the catalyst with Cu/B ratio of 2/1. Higher or lower boron loadings would have great effect on the selectivity of EG, which might be due to the different surface acidities of these catalysts. Based on the NH_3-TPD results, the acid amount increased along with the increase of the boron loading, however, the selectivity of EG did not increase accordingly, which indicated that the proper amount of acidity might greatly improve the product selectivity. Besides the target product EG, the hydrogenation of DMO to produce methyl glycolate (MG) was the main side reaction, and the selectivity of these two products could make 95% contribution in the overall products.

3.5.2. Effect of different boron precursors

To investigate the effect of boron source on the catalytic performance, we carried out the catalytic hydrogenation of DMO reaction over the catalysts modified with different boron sources. Fig. 7(C

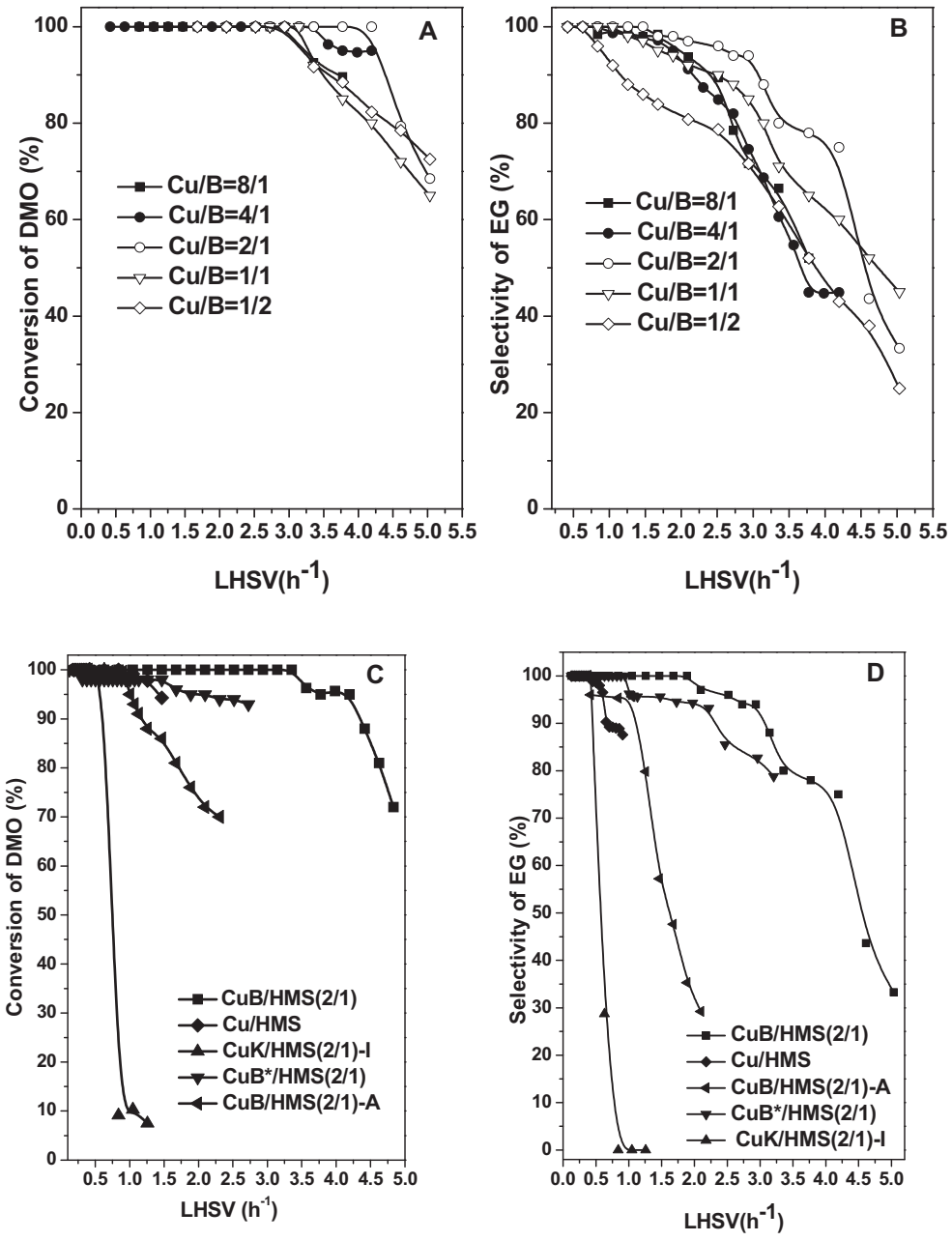

Fig. 7. DMO conversion and EG selectivity of catalysts with different mol ratios of Cu/B (A and B), and catalysts synthesized via different preparation methods and different boron sources (C and D). Reaction conditions: $P = 2.5$ MPa, $T = 473$ K, H_2/DMO = 120 (mol/mol).

and D) depicts the catalytic performance of samples with different boron source modifications. Two main products were MG and EG. Compared with the dramatic effect on the catalytic behavior by changing the Cu/B ratio, the effect of the boron source is much weaker. Under low LHSV conditions (lower than 1.5 h^{-1}), no obvious difference on the DMO conversion and EG selectivity could be observed. The great influence might originate from the synthesis procedure. When one used KBH_4 as boron source, the redox reaction between Cu^{2+} and BH_4^- would happen; Cu^{2+} was reduced to Cu^0 and BH_4^- was changed to B_2O_3, and at the same time the color of the solution changed from deep blue to black; meanwhile, the metallic copper species and B_2O_3 were deposited on the support. It is interesting to find that the fresh metallic copper was reoxidized to Cu^{2+} with the color changing from black to blue after several hours reaction. The bigger particle size (15.8 nm) of the metallic copper species might result from the complex oxidation–reduction procedure, which would lead to the lower hydrogenation conversion and selectivity to EG in comparison with the direct B_2O_3 modified catalyst.

3.5.3. Comparison of different preparation methods

The catalytic performance of the catalyst strongly depends on the preparation method. To investigate the effects of the synthesis method on the catalytic behaviors of the catalysts, two kinds of preparation methods (EVI method and impregnation method) were carried out. The impregnation method is chosen to elucidate whether the dispersion of copper species would be changed upon the catalyst post-modified with B_2O_3. XRD results presented in Table 1 show that the particle size of copper species did not change greatly (4.1 vs 4.7 nm). TPR results shown in Fig. 4 indicate that

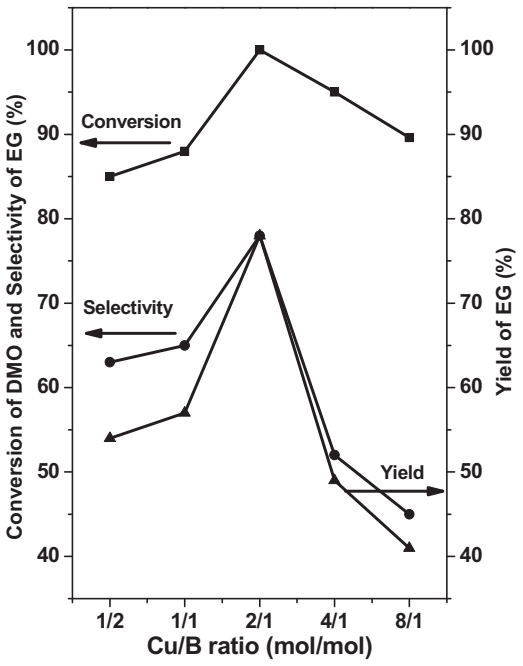

Fig. 8. DMO conversion and EG selectivity of catalysts with different ratios of Cu/B. Reaction conditions: $P = 2.5$ MPa, $T = 473$ K, H_2/DMO = 120 (mol/mol), LHSV = 3.5 h^{-1}.

the dispersion of copper species and the interaction between the copper species and silica support did not change either. Also, the results of NH_3-TPD measurement showed that the overall surface acidity were almost the same. All these results indicated that the differences in the catalytic behaviors of these two catalysts prepared with different methods were not due to the particle size of the active copper species, the dispersion of the copper species or the surface acidity. XPS results showed that the ratio of B/Si (0.104) in the CuB/HMS(2/1)-A sample was much higher than that of CuB/HMS(2/1) (0.064). N_2O titration results presented that the specific surface area of metallic copper of CuB/HMS(2/1)-A sample (9.6 m^2/g) was much lower than that of CuB/HMS(2/1) sample (16.9 m^2/g). Combining the XPS and N_2O titration results, we speculate that the boron species would cover part of the active sites, thus decreasing the specific surface area of the metallic copper species and leading to the decrease in conversion of DMO. In addition, the existence of K species might catalyze the Guerbet reaction into the formation of 1,2-butanediol (1,2-BDO), which would deteriorate the selectivity of EG [5].

The two different preparation methods were also applied in the KBH_4 derived catalysts. Their catalytic performances are also presented in Fig. 7. The dramatic effect on catalytic performance from the two catalysts derived from KBH_4 can be observed. The worse catalytic hydrogenation performance of the catalyst prepared by the impregnation method might mainly result from the larger particle sizes of copper species. In addition, the existence of potassium in the catalyst prepared with KBH_4 impregnating method and detected by XPS might have a side effect on the catalytic performance.

4. Conclusions

In summary, we have studied the catalyst system of boron modified Cu/HMS catalysts. Our findings indicate that the Cu/B ratio has an important effect on the conversion and selectivity for the hydrogenation of DMO. Besides, the different boron sources and different preparation methods could also affect the catalytic behaviors of the catalyst. We observed an increase in dispersion of copper species with increasing boron loading. Also, N_2O titration measurements showed increased specific surface areas of copper species. These two factors lead to the increase in catalytic performance with increasing boron content. However, excessive boron modification caused some non-homogeneity of copper species with lower copper surface areas, leading to the decreased catalytic performance. The highest DMO conversion and EG selectivity could be obtained under the optimized preparation procedure with B_2O_3 as boron source, a Cu/B ratio of 2/1 and EVI method.

Acknowledgements

This work was financially supported by the Major State Basic Resource Development Program (grant no. 2003CB615807), NSFC (Project 20973042), the Research Fund for the Doctoral Program of Higher Education (20090071110011), and the Natural Science Foundation of Shanghai Science & Technology Committee (08DZ2270500).

References

[1] D.S. Brands, E.K. Poels, A. Bliek, Appl. Catal. A: Gen. 184 (1999) 279–289.
[2] L.F. Chen, P.J. Guo, M.H. Qiao, S.R. Yan, H.X. Li, W. Shen, H.L. Xu, J. Catal. 1 (2008) 172–180.
[3] K. Hirai, T. Uda, Y. Nakamura, US4614728 (1986).
[4] H. Miyazaki, T. Uda, K. Hirai, Y. Nakamura, H. Ikezawa, T. Tsuchie, US4585890 (1986).
[5] C. Carlini, M.D. Girolamo, A. Macinai, J. Mol. Catal. A 200 (2003) 137–146.
[6] A.Y. Yin, X.Y. Guo, W.L. Dai, H.X. Li, K.N. Fan, Appl. Catal. A: Gen. 349 (2008) 91–99.
[7] A.Y. Yin, X.Y. Guo, W.L. Dai, K.N. Fan, J. Phys. Chem. C 114 (2010) 8523–8532.
[8] J. Ramirez, P. Castillo, L. Cedeno, R. Cuevas, M. Castillo, J.M. Palacios, A. Lopez-Agudo, Appl. Catal. A: Gen. 132 (1995) 317–334.
[9] J. Fung, I. Wang, J. Catal. 164 (1996) 166–172.
[10] J.G. Wu, M. Saito, H. Mabuse, Catal. Lett. 68 (2000) 55–58.
[11] J. Li, N.J. Coville, Appl. Catal. A: Gen. 181 (1999) 201–208.
[12] S.C. Moon, H. Mametsuka, E. Suzuki, M. Anpo, Chem. Lett. (1998) 117–118.
[13] S.C. Moon, H. Mametsuka, E. Suzuki, Y. Nakahara, Catal. Today 45 (1998) 79–84.
[14] S.C. Moon, H. Mametsuka, S. Tabata, E. Suzuki, Catal. Today 58 (2000) 125–132.
[15] K.Y. Jung, S.B. Park, S.K. Ihmb, Appl. Catal. B: Environ. 51 (2004) 239–245.
[16] P.T. Tanev, T.J. Pinnavaia, Science 267 (1995) 865–867.
[17] Th.J. Osinga, B.G. Linsen, W.P. van Beek, J. Catal. 7 (1967) 277.
[18] G.C. Chinchen, C.M. Hay, H.D. Vandervell, K.C. Waugh, J. Catal. 103 (1987) 79–85.
[19] D.S. Maoa, Q.L. Chen, G.Z. Lu, Appl. Catal. A: Gen. 244 (2003) 273–282.